Optical alignment of the LGS and NGS WFS of ERIS: procedures and first results

Marco Bonaglia[a], Runa Briguglio[a], Luca Carbonaro[a], Paolo Grani[a], Simone Esposito[a], Alfio Puglisi[a], Armando Riccardi[a], and Marco Xompero[a]

[a]INAF - Osservatorio Astrofisico di Arcetri, L.go E. Fermi 5, 50125 - Firenze, Italy

ABSTRACT

ERIS is an adaptive instrument for the UT4 of the Very Large Telescope. It implements both an infrared imager and a spectrograph served by a single-conjugate adaptive optics system able to work with a natural or an artificial guide star. The wavefront correction will be provided by the adaptive secondary mirror of the ESO - Adaptive Optics Facility. The natural and laser guide star wavefront sensors are 2 independent Shack-Hartmann sensors with 40×40 subapertures arranged on CCD220-based detectors provided by ESO. Moreover, each WFS implements an optical device to register the pupil-actuator geometry and to counter-rotate the actuators pattern on the plane of the lenslet array. The NGS WFS also implements a low-order sensor with 4×4 subapertures to work as tip-tilt and truth sensor during the LGS operation.

Both the LGS and NGS WFS units of ERIS are now completing their assembly and integration phase in laboratory at the Arcetri Observatory. We present in this paper the procedures we employed to optically align the 2 WFS units, discussing the precision we achieved in the process. Such alignment concept was successfully proven in the FLAO Pyramid WFS and we expect to be able to adopt it also for the Low-Order and Reference (LOR) WFS of MAORY for the ELT.

Keywords: single conjugate adaptive optics, Shack-Hartmann wavefront sensor, natural and laser guide star, Very Large Telescope

1. INTRODUCTION

The Enhanced Resolution Imager and Spectrograph (ERIS)[1] is an adaptive instrument for the Unit Telescope 4 (UT4) of the Very Large Telescope (VLT) at the Paranal Observatory. It is made of three main components: NIX, SPIFFIER and the Adaptive Optics Module (AOM). NIX[2] is a replacement for NACO, it provides an infrared imager working between 1 and 5 μm with coronographic capabilities. SPIFFIER[3] is an integral field spectrograph with a wavelength coverage of 1-2.5 μm and a spectral resolution R ~ 4000. It is mainly a refurbishment of SPIFFI. The AOM[4] is a single-conjugate AO system working either with a natural guide star to ensure high-contrast correction or an artificial guide star to maximize the instrument sky-coverage.

The AOM is taking full advantage of the Adaptive Optics Facility (AOF)[5] built by the European Southern Observatory (ESO) and installed at UT4 in 2017. Indeed the AOF provides ERIS with both a wavefront corrector, the Deformable Secondary Mirror (DSM)[6], and a laser guide star projector, which can be one of the four launchers of the 4LGSF[7] system. Moreover ERIS makes use of the detector and real-time-computer technology developed at ESO for the GALACSI and GRAAL instruments: the CCD220-based wavefront sensor cameras[8] and a modified version of SPARTA[9].

An overview of ERIS is shown in figure 1. The AOM itself is made out of four main components:

- The "warm optics": a set of optical components, that relay the telescope optical beam out from the Cassegrain Flange to the science instruments and to the two WFSs.
- The LGS WFS: an high-order Shack-Hartmann sensor (SHS) with a pupil sampling of 40×40 subapetures, a field of view (FoV) equivalent to 5 arcsec on-sky and 6×6 pixels per subaperture (~ 0.8 arcsec/pixel scale). It operates only with an on-axis LGS, so it requires only an active compensation for the Sodium layer height.
- The NGS WFS: it accomplishes both high-order (HO) and low-order (LO) functionality for standard NGS operation and LGS operation respectively. In the first case the configuration is similar to the LGS WFS: 40×40

subapetures, 6 × 6 pixels per subaperture, but it has a reduced FoV equivalent to 2.5 arcsec (so ~ 0.4 arcsec/pixel scale). In the low-order mode the WFS is configured to have 4 × 4 subapetures sampled with 12 × 12 pixels hence having a ~ 0.2 arcsec/pixel scale). Moreover, to ensure an adequate sky-coverage, the NGS WFS has to patrol a 120 arcsec diameter circular-area on the telescope F13.4 focal plane to pickoff a NGS.

- The calibration unit[10]: it provides facilities to calibrate both the scientific instruments and to perform troubleshooting and periodic maintenance tests of the AO WFSs and the science instruments.
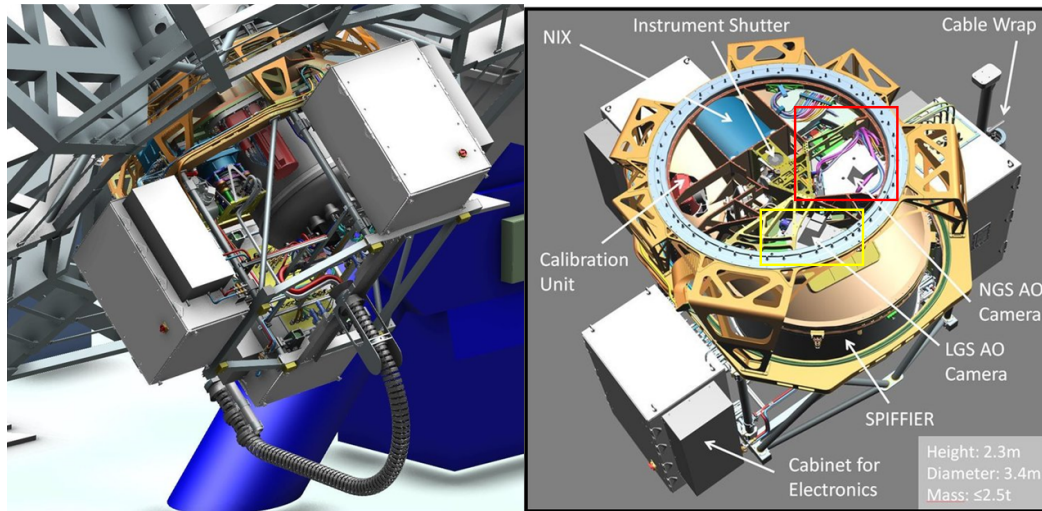

Figure 1. Left: 3D model of ERIS mounted at the Cassegrain focus of VLT-UT4. Right: detail view or ERIS as seen from the top of the AOM. The NGS and LGS WFSs are highlighted by the red and yellow boxes respectively. Credits MPE.

2. LAYOUT OF THE LGS AND NGS WFS

The layout of the 2 WFS is very similar: both units are provided with a focus compensation stage to reduce the non-common path aberrations with the instrument, a pupil steering mirror to preserve the actuator-subaperture registration and a K-mirror mounted on a rotary stage (Physik Instrumente L-611) to track the actuators pattern while the field is derotated. The WFSs optical paths are made out of an input triplet, working close to a 2f-2f configuration, and a collimator to relay the input pupil on the lenslet array. In both WFSs the pupil steering mirrors (Physik Instrumente S-334) are positioned in (or close to) the intermediate focal plane provided by the input triplet lens.

The difference in the opto-mechanical arrangement of the LGS and NGS WFS can be noticed from the schematics and pictures reported in figure 2. The increased complexity of the NGS WFS is due to:

- A 32 mm long periscope mounted on a rotary stage. It is required to allow for field patrolling along the vertical direction, with respect to the optical breadboard. Indeed the limited volume available within the AOM structure prevented the usage of dual-axes stage for field patrolling. Moreover, to make the WFS board even more compact, the input triplet is glued on the first surface of the periscope.
- An Atmospheric Dispersion Corrector (ADC). The ADC is required to minimize the size of the telescope PSF on the WFS internal focal plane, to allow to implement a spatially filtered SHS, through a variable iris in the internal focal plane. This allows to enhance the WFS sensitivity in the bright end regime.
- A beam splitter dichroic transmitting wavelengths shorter than 600 nm towards a technical camera that can be used both for calibration/maintenance purposes and for the on-sky NGS acquisition.
- A filter wheel hosting a beam stop for dark calibration, a pass-all filter for normal operations and two ODs to reduce the light level and avoid over-illumination in case of bright NGS.

- A linear stage to switch between HO and LO configurations (HoLo switch). On top of it the lenslet arrays are mounted into 2 barrels with a doublet lens. Downstream of the switch a second doublet produces a 1:1 relay of the SH pattern on the WFS camera.
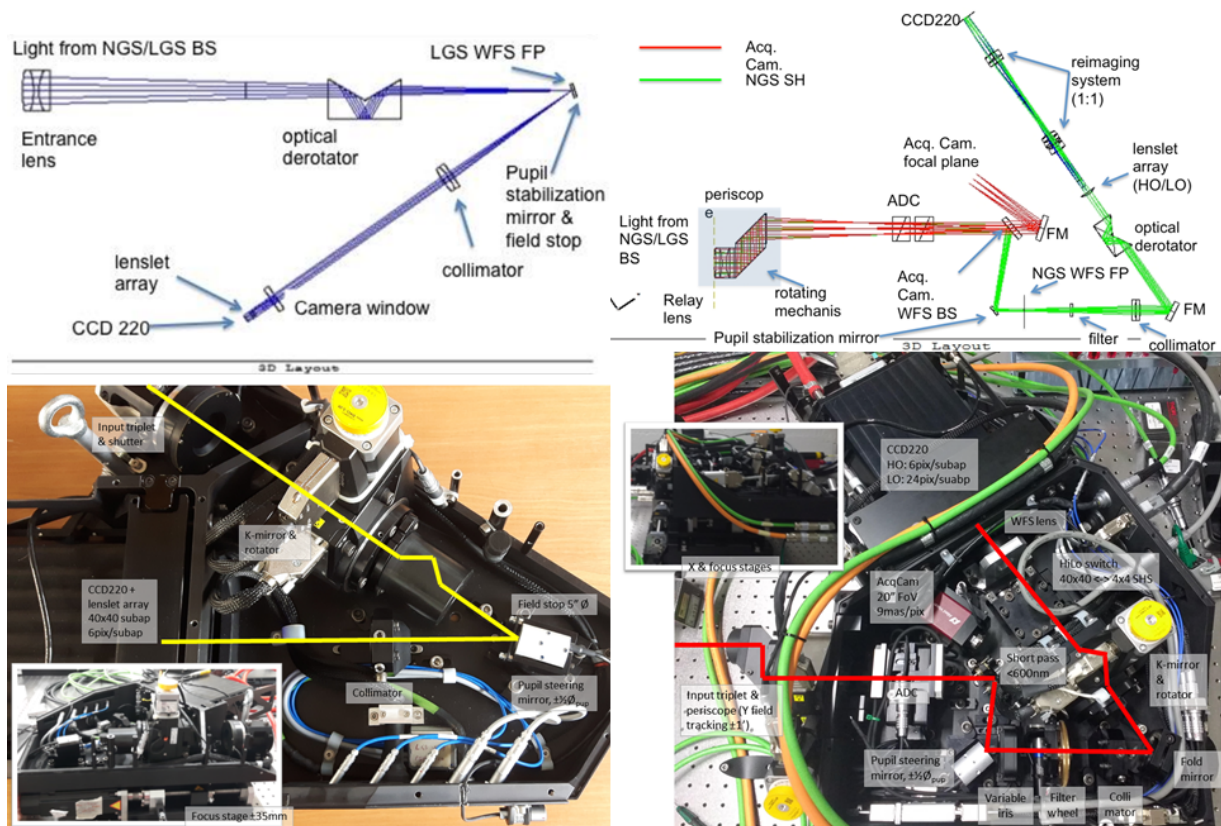

Figure 2. Summary of the optical (top) and mechanical (bottom) layouts of the LGS and NGS WFS. The first one is shown on the left and it is a way more simple than the NGS one, shown on the right. The input lens works close to a 2f-2f configuration producing an internal focal plane where a pupil steering mirror and a field stop are placed. Then a collimator relays the input pupil on the lenslet array. In the LGS WFS the K-mirror takes place in the convergent beam while in the NGS one is in the collimated beam. Moreover the NGS WFS is provided with an ADC, an acquisition camera and a set of relay optics to switch between the 40 × 40 subapertures high-order sensor and the 4 × 4 low-order one.

3. ACTUATORS ASSEMBLY AND TEST

The first step of the WFS integration has been to assemble the complex opto-mechanical devices, like the ADC, the pupil rotators, the NGS periscope and the HoLo switch. These devices put together a series of optical elements (e.g. prisms and lenses) within a single mount and a remotely controlled actuator (e.g. rotary or linear stages). Most of these devices do not require a tight alignment tolerance and they have just been tested for the mechanical stresses using an interferometric setup. However in the case of the pupil rotators the optic mount is provided with manual adjustment screws to finely align the optical assembly with respect to the actuator rotation axis. The next section focuses on the assembly and verification procedures for these devices. The control algorithms for the actuators and their driving electronics are described in a dedicated paper[11].

3.1 Pupil rotators internal alignment

The pupil rotators are realized through a K-prism, implemented with an Abbe prism, rotated by a Physik Instrumente (PI) rotation stage L-611. We integrated and aligned two units, respectively for the LGS and NGS WFS boards. The alignment procedure consists of minimizing the wobble of the spot produced by a point source placed before the K-mirror, when the system is rotated. The resulting beam wobble could be due to a relative angle between the axis of the optic component and the rotator one, or a decenter error between the optic axis and the reference beam. The alignment procedure is based on a first step to adjust the stage orientation with respect to a given reference axis, which is conveniently materialized by the interferometer laser beam. In a second step the system center is identified. In the last step the optics are aligned and centered. The breakdown of the alignment procedure is the following:

1. the rotation stage is placed in front of an interferometer with the rotation axis roughly parallel to the optical axis; a flat mirror is placed on the rotation platform to have a return beam on the interferometer screen. the mirror is aligned to have a decent alignment for any rotation angle of the stage. A calibrated stop (e.g. 5 mm) is placed at the interferometer output.
2. the stage is rotated by 360° and an interferometer frame is captured at any angle; each frame is analyzed to measure the tip/tilt and compute the beam deviation.
3. the tip values are plotted against tilt to visualize the resulting circle, whose radius is the mirror mis-alignment (to be neglected) and whose center with respect to [0;0] is the rotator off-axis.
4. the rotator is aligned to place the resulting circle at [0;0] center.
5. the mirror is removed and a pinhole is installed on the rotation platform (no centering accuracy is required); a camera is installed after the rotator;
6. the rotator is rotated and the position of the pinhole spot is measured on the camera. the center is computed to visualize the rotation axis intersect at the camera.
7. a pinhole is placed on an XY stage installed on the interferometer output flange; the pinhole is adjusted to have the spot at the rotation center; the mounting repeatability is checked, then the pinhole is removed;
8. a flat mirror is installed after the rotator and aligned with the interferometer;
9. the K-mirror is installed in the rotator and placed with the fast axis vertical; it is then and aligned with the interferometer: the vertical tilt measured on the flat mirror shall be opposite after 180° rotation.
10. the centered pinhole is installed back and its spot is measured on the camera after a complete revolution; the K-mirror is centered to minimize the spot wobble.
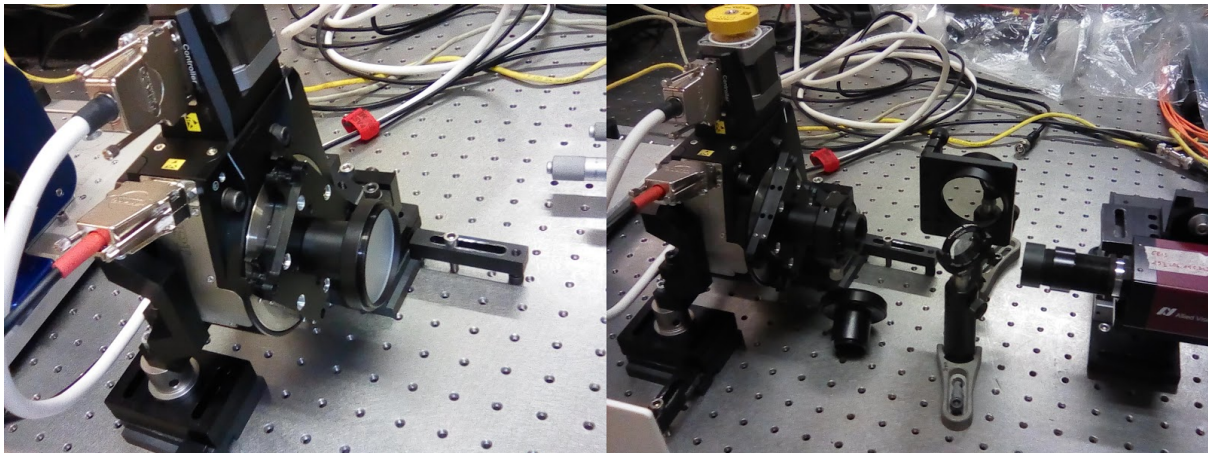

Figure 3. Left: rotation stage with flat mirror attached on the platform for the rotator alignment to the reference beam produced by the 4D interferometer (steps #1-4). The interferometer is on the left side, outside picture. Right: optical setup with a pinhole, camera and flat reference mirror to identify the rotator center (steps #5-8).

4.   LGS AND NGS WFS INTERNAL ALIGNMENT

This section describes the internal alignment of the 2 WFS boards. In a nutshell, the optical alignment goal is to position the axes of the pupil rotators at the center of the SHS subapertures. This is required to minimize the wobble of the pupil and the science images when the adaptive optics loop is closed. The first error is compensated actively by an internal control loop to the WFS, that actuates the pupil steering mirror relying on the pupil position as measured by the real-time computer. The requirement on the alignment error residual is set to avoid compromising the dynamic range of the actuator, basically a ± 1 subaperture pupil wobble can be tolerated.

The image wobble on the WFS focal plane instead induces a non-common path error with the science instruments. This effect has to be mitigated by applying pointing offsets to the WFS through a pre-calibrated lookup table (LUT). In this case, the requirement on the alignment error residual is stringent, especially in the case of the NGS WFS. The ERIS image motion budget allocates to the pupil rotator of the NGS WFS, before LUT is applied, a maximum error of 0.56 mas per degree of the instrument rotator. This is equivalent to an image wobble of 50 mas for a 90° rotation of the sky that corresponds to 1 hour of observation at $z = 6.5°$. In the LGS WFS case the image wobble requirement can be relaxed since the system has the possibility to actively compensate for the LGS position by adjusting the launch optics. A PSF wobble error equivalent to a peak-to-valley (PtV) displacement ~ 1 arcsec on-sky can be tolerated in the LGS WFS.

The pupil rotator axis is defined as a combination of the rotary stage mechanical axis and the K-mirror axis in such a way that minimizes both the PSF wobble and the chief-ray tilt of the emerging beam. The subaperture centre is simply identified by the position that minimizes the average tip and tilt signals as measured by the WFS. This result is achieved using common tools, procedures and optical references, like:

- the beam projectors. They are portable collimated lasers used as light sources. During the alignment process they replace the input lens, sitting on the V-block of the LGS WFS or attached to the periscope rotator of the NGS WFS.
- A centering tool acting as a reference in the XY plane (where Z is the direction of the light propagation). On its front flange, it has a mark at the nominal beam height (60 mm). On the baseplate, it also has a cut to fit on top of the rail system of both breadboards.
- A back-reflecting mirror used to null the tip-tilt errors with respect the rails and board system. It is mounted on a L-shaped bracket having a cut on the baseplate to fit on top of the board rails.
- An alignment camera with 2040 × 2040 pixels of 7.4 μm size. This is an Allied/AVT GE2040 with Ethernet interface, namely the same used as acquisition camera in the NGS WFS.

4.1 LGS WFS alignment

The peculiarity of the LGS WFS is that the lenslet array is glued on top of the chip package, inside the camera housing. Because of this, the fine positioning of the pupil rotator axis within the subaperture is achieved tilting the whole WFS camera assembly in pitch and yaw. The main steps of the LGS WFS internal alignment are the following:

1. The pupil rotator axis has to coincide with the pointer beam.
2. The pointer beam reflected by the pupil steering mirror has to be parallel to the camera lens rail and to the WFS breadboard.
3. The WFS camera pixel array must be centered on the pointer beam.
4. The collimator must preserve the beam position on the WFS camera.

The pupil rotator is the first element that is aligned on the LGS WFS board. Previously it was verified that installing and removing the K-mirror from the rotary stage interface did not impact the alignment of the optical assembly to the mechanical axis of the rotator. So to align the rotator axis to the pointer beam the K-mirror is removed. To have a reference for the alignment in tip-tilt, a sheet of paper with a tiny hole is stuck on the V-block holding the pointer beam. The back-reflection on the paper sheet is obtained by sticking a flat mirror on the back surface of the rotator. The

expected resolution is not better than 0.25 mm, but it is sufficient in ensuring that a ± 1.2 mrad residual tip-tilt error is achieved (the mirror is placed at 208 mm distance from the V-block). This value can be accepted because it is comparable with the ± 1.75 mrad beam deviation induced by the LGS K-mirror, due to the angle error between the reflecting surfaces introduced during the glueing of the 2 optic components. The residual beam deviation will be actively compensated during the ERIS LGS operations by closing the internal control loops that adjust the pupil steering mirror and the LGS launcher positions.

To measure the decenter error of the pupil rotator the alignment camera is positioned downstream of it. The reference position of the pointer beam is acquired on the camera and then a pinhole is attached to the rotator, see FIGURE. The pinhole is moved at the center of the rotator using fine adjustment screws and nulling the variation in the spot position measured when the rotator is moved at 90° steps. Reaching a 10 μm accuracy on the spot position on the camera is trivial. Considering a 100 mm distance from the pinhole and the camera, the residual decenter error on the pupil rotator produces a 0.1 mrad of beam deviation, that is negligible with respect to the tip-tilt component.
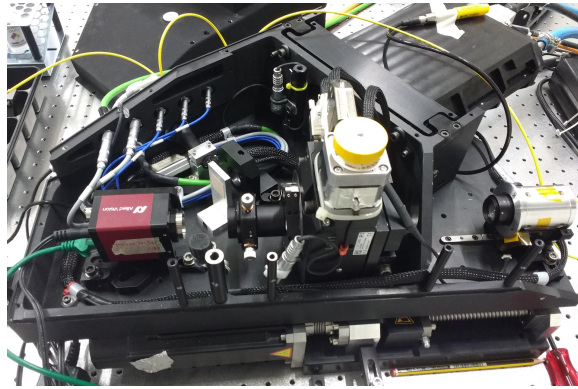

Figure 4. Picture of the LGS WFS board during the pupil rotator alignment in decenter. The K-mirror was removed and a pinhole was mounted on the rotary stage (PI L-611). The feedback for the alignment process was given by the alignment camera mounted downstream of the rotator. On the right of the picture, it is visible the V-block holding the laser pointer.

The alignment of the pupil steering mirror is performed in 2 steps: at first the "nominal" position of the piezo actuators is recorded, then the mirror mount is slid along the rail to center the reflected beam on the collimating lens rail. The piezos "nominal" positions are basically the DC offsets that must be applied to the amplifiers to back-reflect the pointer beam on itself, as reflected by the alignment mirror on the paper sheet. Considering a 345 mm distance from pupil steering mirror and the V-block, a residual tip-tilt error of ± 0.72 mrad is expected. Since the PI S-334 tip-tilt platform allows for a 100 mrad beam steering over a 0 - 10 V DC input command, the residual alignment error translates to a ± 0.05 V uncentanty on nominal position recorded for the piezos.

The position of the pupil steering mirror along its rail is determined by looking at the spot position on the centering tool positioned in front of the collimating lens mount. A 0.25 mm resolution can be reached in this process by taking pictures of the spot on the target, however this decenter error does not impact the LGS WFS performance since all the optical elements downstream of the pupil mirror (collimator and WFS camera) are provided with decenter adjustments.

To align the WFS camera in the XY plane the pinhole is kept in position on the PI rotator, to produce a larger and more uniform illumination pattern on the detector ($\sim 15 \times 15$ subapertures). To center the WFS camera on the pointer beam the XY adjustment screws on the camera mount are used and the feedback is given by the total flux evaluated in the subapertures. With this configuration reaching a 1/10 subap resolution is possible. Then the average tip-tilt component measured on the limited number of subapertures illuminated by the pointer beam has to be nulled by tilting the WFS camera assembly. These 2 steps must be iterated, to refine and to cross-check the alignment output. The balancing between the subaperture illumination and the spot positions was done by-eye, looking at camera Real Time Display

(RTD) as shown in figure 5. Considering a 1/10 pixel resolution, the nominal 0.83 arcsec/pixel scale of the LGS WFS, the residual tip-tilt expected from the WFS camera alignment is equivalent to ± 83 mas on-sky.
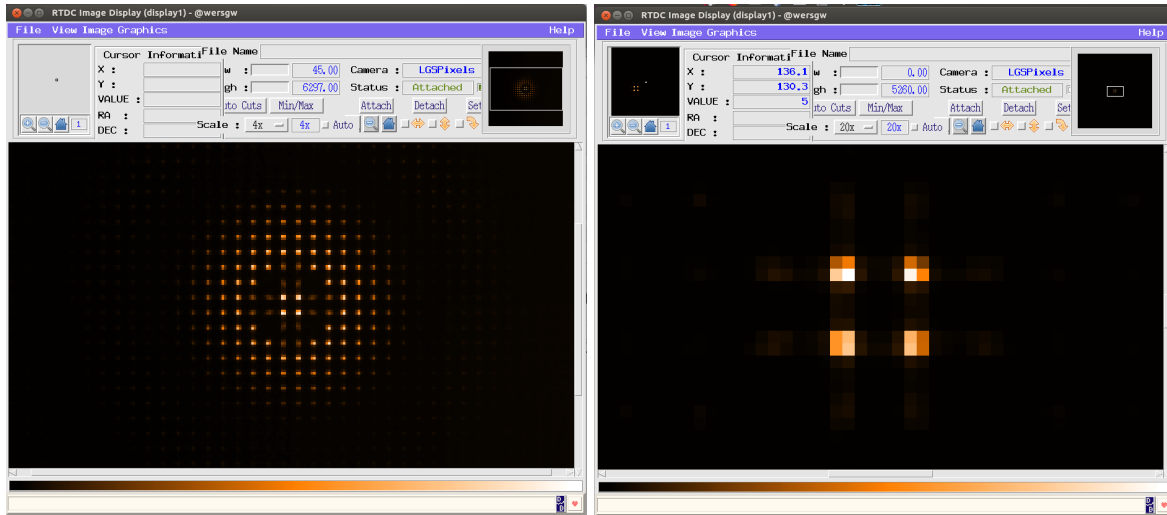

Figure 5. Screenshots of the camera RTD during the alignment in decenter (left) and tip-tilt (right) of the assembly.

In the end the collimating lens is placed on the WFS board. Its mount is provided with a fine-adjustment in XY through a couple M5 screws. The lens must be inserted in the optical path in such a way to not modify the beam position and average tip-tilt signals as measured on the LGS WFS. The feedback for the collimating lens alignment is given by the same tools used to align the WFS camera, hence the same accuracy level is expected. Table 1 resumes the output of the LGS WFS alignment process and it summarizes the effect expected on the pupil and focal planes. In the specific case of the ERIS LGS operation these 2 values translate into a continuous offset to the pupil steering mirror and the LGS launch optics driven by the internal control loops to the AOM.

Table 1. Summary of the error sources in the LGS WFS internal alignment and effects expected on the focal and pupil planes. To evaluate the effects of the residual alignment errors on the focal and pupil planes, nominal distances have been considered: pupil rotator lays at 78 mm from the FP and 112 mm from the PP, while the PSM is at 237 mm from the PP.

Element	Residual error	Focal plane	Pupil plane
Pupil rotator	Tip-tilt: ± 1.2 mrad	± 118 mas	± 0.45 subap
	Decenter: ± 0.1 mrad	± 10 mas	± 0.04 subap
	K-mirror: ± 1.75 mrad	± 173 mas	± 0.65 subap
Pupil steering mirror	Tip-tilt: ± 0.72 mrad	-	± 0.57 subap
WFS camera	Tip-tilt: ± 0.1 pixel	± 83 mas	-
	Decenter: ± 0.1 subap	-	± 0.10 subap
Collimator	Dec.: ± 0.1 pixel and ± 0.1 subap	± 83 mas	± 0.10 subap
	Total (square sum)	**± 240 mas**	**± 0.98 subap**

4.2 NGS WFS alignment

In the NGS WFS the Shack-Hartmann lenslet arrays and the WFS camera are obviously decoupled to allow switching between the 40×40 HO sensor and the 4×4 LO one. However most of the optical elements are in common path, hence the internal alignment of the NGS WFS can be summarized in the following steps:

1. The pointer beam is made parallel to the board and coincident with the rails (up to the pupil rotator) using the centering tool (XY) and the reference mirror (tip-tilt).
2. The WFS camera is centered on the pointer beam.
3. The collimating lens is aligned on the pointer beam.
4. The pupil rotator is aligned in tip-tilt looking at the back reflection of the pointer beam from the first surface of the K-mirror and adjusting the fold mirror in tip-tilt.
5. The pupil rotator is centered on the pointer beam nulling the beam wobble on the alignment camera, positioned downstream of the pupil rotator, by adjusting the fold mirror position along the rail (X) and the pupil rotator mount in height (Y).
6. The WFS lens is displaced to move the rotator axis on the subaperture center.
7. The variable iris is centered on the pointer beam.
8. The HoLo switch is aligned on the pointer beam.

All these points are detailed in this section. However the ADC, periscope and filter wheel do not have degrees-of-freedom for the optical alignment, hence they are placed in their nominal position at the end of the alignment procedure.

The acquisition camera alignment is trivial since it just requires the compensation of the differential focus with respect to the SHS sliding along the optical axis.

The first three optical elements that are positioned on top of the NGS WFS board are just flat mirrors: the dichroic, the pupil steering mirror and the fold mirror. They are aligned in tip-tilt in such a way to back-reflect the pointer beam on itself and to make the pointer beam parallel to the rail system, when the back-reflecting mirror is inserted downstream of them. Their position along the rail system are corrected by using the centering tool. As in the LGS WFS alignment the visual feedback on the beam tip-tilt error is given by a sheet of paper, with a tiny hole in the middle, stuck on the periscope support flange. So 0.25 mm resolution is considered in the tip-tilt alignment of the NGS WFS flat mirrors. The residuals of the alignment errors expected are summarized in table 2. Pictures taken during the alignment process of the NGS WFS folders are shown in figure 6.
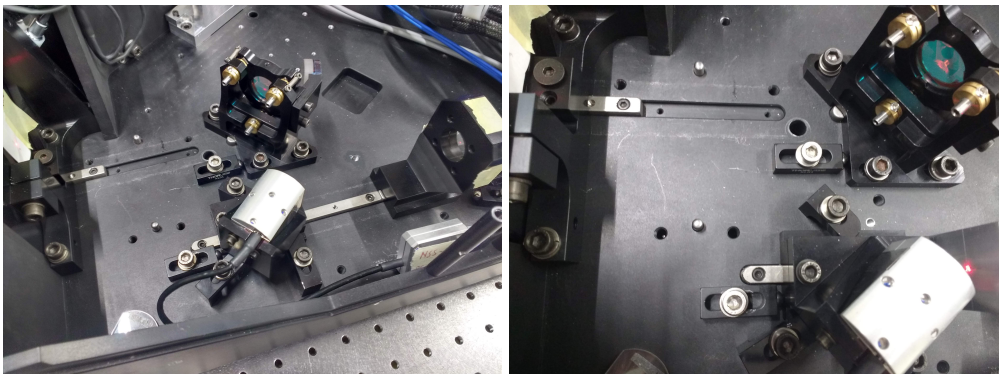

Figure 6. Pictures of the folders alignment on the NGS WFS. Left: the back-reflecting mirror is inserted downstream of the dichroic and the pupil steering mirror to null the tip-tilt error. The visual feedback for the alignment is given by the spot position as seen on the paper screen attached to the periscope flange on the left side of the picture. Right: the centering tool is used to null the decenter error with respect the nominal beam height and the rail direction.

The WFS camera is aligned to the pointer beam by looking at the CCD viewer and adjusting the decenter screws on its mount to bring the spot at the center of the pixel array. This procedure relies on the visual feedback provided by the WFS camera RTD, but a 1/10 pixel resolution can be achieved in the process.

The collimating lens is then inserted in the optical train and its position is adjusted in XY acting on two M5 screws on the lens holder. The feedback still comes from the spot position on the RTD and the target position is still the center of the chip. Once the collimator is aligned at the level of 1/10 pixel with respect to the pixel array, all the optical elements up to the pupil rotator are fixed, so the next step is to mutually align the pupil rotator and the pointer beam. Being placed before the pupil rotator, all the elements installed so far on the breadboard do not contribute to the pupil or image wobbles.

To internally align the K-mirror with respect to the rotator axis at arcsecond level a complex procedure using the 4D interferometer was set up, as detailed in section 3.1. Since it was verified that the internal alignment of the pupil rotator was not preserved if the K-mirror was dismounted and mounted back again on the rotary stage, the alignment procedure of the NGS rotator has to be different from the LGS one.

The feedback on the alignment in tip-tilt of the rotator axis is given by the back reflection of the pointer beam on the K-mirror first surface, as seen on the paper screen on the periscope flange. The compensation of a tip-tilt error between the pointer beam and the NGS rotator is done acting on the fold mirror rotation (to adjust the "in plane" angle) and the adjustment screws of the NGS rotator mount (to adjust the vertical angle with respect to the breadboard). Considering a 547 mm distance between the pupil rotator and the paper sheet, the expected residual for the tip-tilt alignment is ± 0.46 mrad (see table 2). Because the HO lenslets have a focal length of 8.29 mm, the tip-tilt residual translates into an image wobble on the SHS of ± 3.8 μm (or ± 0.16 pixels), equivalent a circle with 66 mas radius on-sky (the nominal plate scale for the HO case is 0.417 arcsec/pixel). Under these assumptions a 45° motion of the NGS pupil rotator will induce an image displacement of ¼ π R = 52 mas, that is compliant with the requirements set by the ERIS image motion budget.

Table 2. Summary of the residuals expected in the tip-tilt alignment of the NGS WFS elements.

Element	Distance to screen	Residual error
TV dichroic	237 mm	± 1.05 mrad
Pupil steering mirror	316 mm	± 0.79 mrad
Fold mirror	491 mm	± 0.51 mrad
Pupil rotator	547 mm	± 0.46 mrad

To co-align the NGS rotator and the pointer beam, nulling their decenter error, the alignment camera was installed after the NGS rotator (e.g. on top of the HiLo switch mount, as shown in figure 7). Indeed the feedback to align the decenter component is given by the beam wobble as measured on the alignment camera, when the pupil rotator is spinned. The measurement procedure is the same used to align the rotator assemblies with the 4D interferometer. The decenter corrections are applied on two different degrees of freedoms: the fold mirror was slid along its rail to null the X component, while the Y component was corrected by turning the adjustment screws of the NGS rotator mount. The residual measured on the alignment camera amounts to 160 μm PtV (see right plot in FIGURE). Considering a 100 mm distance between the pupil rotator and the alignment camera the residual decenter alignment error amounts to ± 65 μm. Because the pupil rotator lays in a collimated beam the effect on the focal plane is negligible. On the pupil plane, however, a ± 1.1% pupil wobble is expected (or ± 0.45 subaperture in the HO case, considering a 5.76 mm diameter pupil). This error will be mitigated by the internal pupil control loop of the NGS WFS.
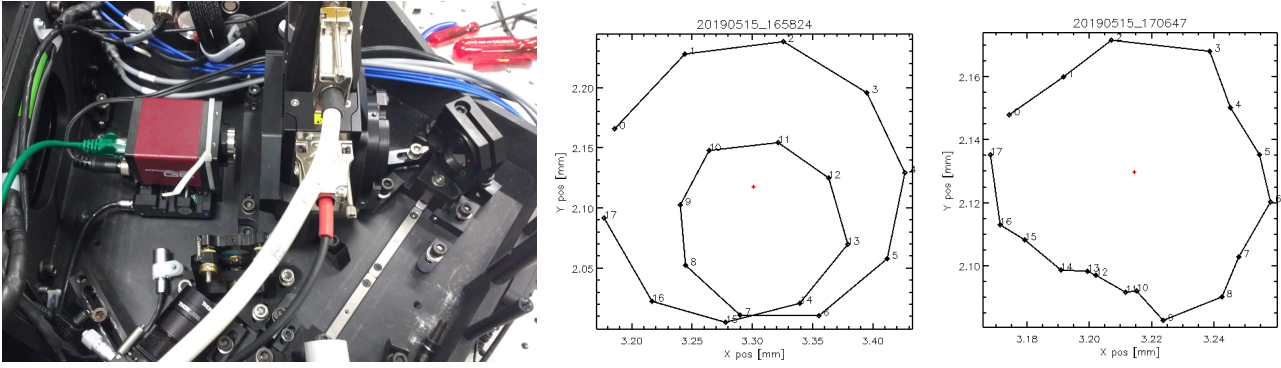
Figure 7. Left: picture of the pupil rotator alignment on the NGS WFS. The acquisition camera was temporary fixed on top of the HoLo switch. Right: output of the procedure to measure the beam wobble before and after the alignment is completed. The cardioid pattern (left plot) highlights a misalignment between the beam projector and the pupil rotator that must be corrected with the co-alignment. The single circle measured after a full 360° spin of the pupil rotator (right plot) is the residual of the alignment procedure and it identifies an internal misalignment of the NGS pupil rotator assembly (e.g. K-mirror axis with respect to the rotary stage axis).

The WFS lens is used to fine tune the beam position on the WFS camera, and hence to center the pupil rotator axis position with respect to the pixel array. This lens is provided with a couple of XY fine-adjustment M2.5 screws. The feedback is given by the RTD where the ~ 2 mm diameter pointer beam is imaged in less than 1 pixel by the WFS lens, having a 47 mm focal length.

The last element to be aligned on the NGS WFS board is the HoLo switch. The feedback to the alignment process is given by the spot pattern on the RTD. The optic mount is provided with 2 sets of adjustment screws that allow to move independently the 2 barrels in pitch and yaw. The front set of screws is positioned in correspondence of the lenslet arrays and allows to balance the illumination pattern: basically they move the lens pattern with respect to the pointer beam. The second set of screws is positioned close to the relay lenses and they allow to fine tune the spot position within the subaperture, by introducing a slight tip-tilt in the refracted beam.

In the end the clock of the SH spots with respect to the pixel array is corrected adjusting the barrel roll. Indeed the 2 barrels are provided with an independent pinion gear on the common mount. Due to the limited number of subapertures illuminated by the pointer beam the residual clock error is in the range of 0.1 - 0.2° in the LO and HO cases respectively, that is equivalent to 1/10 pixel resolution over a 5 subapertures (0.144 mm pitch) baseline, in the HO case, and 1 subaperture (1.44 mm pitch) in the LO case. So the alignment of this degree of freedom must be refined once the full pupil will be illuminated, using the calibration unit as light source.

5. INTERNAL ALIGNMENT VERIFICATION

The quality of the two WFS internal alignment is verified using the calibration unit. This light source allows to mimik the telescope focal plane and exit pupil position so that the full 40 × 40 subapertures are uniformly illuminated, as shown in FIGURE. The goal of the alignment process is to minimize two effects:

1. the pupil and image motions introduced by a mismatch between the reference (or telescope) optical axis and the pupil rotator axis,
2. the static offset between the two centers: i.e. the center of the rotation pattern and the center of the subaperture. This is introduced by a mismatch between the pupil rotator axis and the subaperture center.

Both the NGS and LGS WFS are provided with an automatic software procedure (template[12]) that measures these two effects. The software script configures all the WFS internal actuators for their "nominal" position, as recorded at the end of the optical alignment procedure, and then it setup the light sources to mimic an NGS, an LGS or both of them. In the

end the template records both the WFS signals and the pupil positions while the pupil rotator is moved (e.g. at 30° steps). The output of the template for the LGS and NGS WFS are shown in figure 8.

In the LGS WFS the PtV of the pupil wobble amounts to 2.5 subapertures, while the PSF wobble amounts to 0.46 pixels. These results are compliant with the output of the alignment errors summarized in table 1: ~ 2 subap PtV and ~ 0.6 pixels, considering the nominal 0.833 arcsec/pixel scale.

In the NGS WFS the PtV of the PSF wobble amounts to 0.07 pixels, that is 4 times less than what we expected from the alignment error estimation performed in section 4.2 (± 0.16 pixels). This implies that the resolution we could achieve taking pictures of the back-reflected spot on the paper sheet could be better than 0.25 mm (e.g. 0.1 mm). Considering the nominal plate scale of 0.417 arcsec/pixel the PSF wobble is equivalent to ~ 30 mas on-sky, measured over a full revolution of the instrument rotator. This value is compliant with the image motion budget of ERIS, that allowed for a 50 mas image wobble for a 90° rotation (equivalent to 1 hour of observation at z = 6.5°). The [0.22; -0.11] pixels distance measured from the center of the rotation pattern to the center of the subaperture is equivalent to have a ~ 100 mas offset in the "reference" signals of the NGS WFS. This value has been considered acceptable in terms of impact on the operation performances.
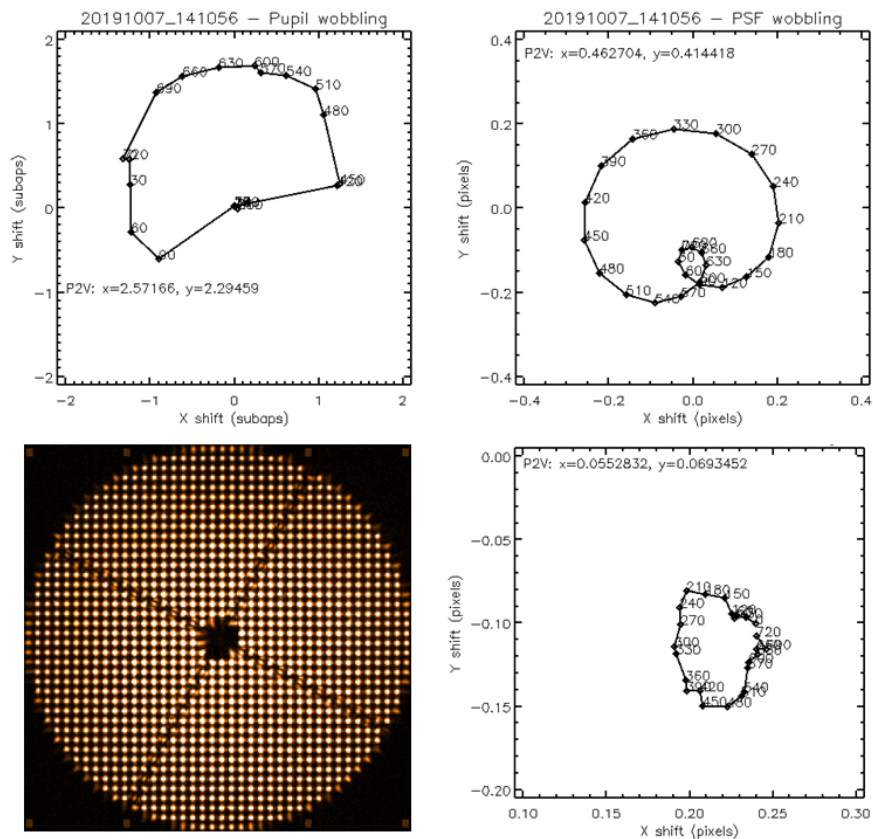

Figure 8. Top row: plots of the data measured by the LGS WFS template for the pupil (right) and PSF (right) wobbles. Bottom row, left: image recorded on the detector of the NGS WFS with the calibration unit. Right: plot of the PSF wobble recorded by the instead the data obtained in the template

6. CONCLUSIONS

The paper focuses on the description of the internal alignment for the LGS and NGS WFS of the ERIS Adaptive Optics Module. Shortly, both WFSs are provided with a K-mirror mounted on a rotary stage to provide an active pupil rotation device, able to preserve the actuator-subaperture registration while field tacking is activated.

The aim of the alignment is to match the optical axis of the pupil rotator with the subaperture center. Both the tools and the procedures used in the alignment process have been detailed in section 4. The various error sources and their contribution have been analyzed, producing an estimation for the pupil and PSF wobbles expected on the two WFS. The values measured at the end of the alignment process are compliant with the system specifications, as demonstrated in section 5.

REFERENCES

[1] Davies, R., et al. "ERIS: revitalising an adaptive optics instrument for the VLT," Proc. SPIE 10703 (2018).

[2] Taylor, W. D., et al. "NIX, the imager for ERIS: the AO instrument for the VLT," Proc. SPIE 9909, p. 99083F (2016).

[3] George, E. M., et al. "Making SPIFFI SPIFFIER: upgrade of the SPIFFI instrument for use in ERIS and performance analysis from re-commissioning," Proc. SPIE 9909, p. 99080G (2016).

[4] Riccardi, A., et al. "The ERIS adaptive optics system: from design to hardware", Proc. SPIE 10703, id. 1070303 (2018).

[5] Madec, P.-Y., et al. "Adaptive Optics Facility: from an amazing present to a brilliant future," Proc. SPIE 10703 (2018).

[6] Briguglio, R., et al. "The deformable secondary mirror of VLT: final electro-mechanical and optical acceptance test results," Proc. SPIE 9148, p. 914845 (2014).

[7] Hackenberg, W. K., et al. "ESO 4LGSF: Integration in the VLT, Commissioning and on-sky results," Proc. SPIE 9909 (2016).

[8] Downing, M., et al. "AO WFS detector developments at ESO to prepare for the E-ELT", Proc. SPIE 9909, id. 990914 (2016).

[9] Suárez Valles, M., et al. "SPARTA for the VLT: status and plans", Proc. SPIE 8447, id. 84472Q (2012).

[10] Dolci, M., et al. "Final design and construction of the ERIS calibration unit," Proc SPIE 10702 (2018).

[11] Grani, P., et al. "Verification and Acceptance Test Results of the ERIS Adaptive Optics Module Mechatronics", this conference.

[12] Baruffolo, A., Salasnich, B., "Design of the ERIS instrument control software," Proc. SPIE 10707 (2018).